

On the Role of Cloud Amount in an Energy Balance Model of the Earth's Climate

H. M. VAN DEN DOOL

Royal Netherlands Meteorological Institute, De Bilt, The Netherlands

(Manuscript received 14 August 1979, in final form 17 January 1980)

ABSTRACT

The influence of cloud amount on the earth's climate is studied with an energy balance climate model. Planetary albedo and infrared radiation are parameterized in terms of cloud amount and surface temperature. For the present climate a prescribed change in cloud amount (independent of latitude) leads to a negligible change in the global mean temperature ($\partial T/\partial A_c \approx 0$). For global temperatures lower than present $\partial T/\partial A_c$ becomes positive rapidly; higher temperatures lead to negative values of $\partial T/\partial A_c$. The sensitivity of the global mean temperature to a 1% change in the solar constant ($\partial T/\partial S$) is ~ 1.5 K. With reduced cloud amount $\partial T/\partial S$ becomes larger because the snow-ice feedback is active in the larger cloud-free portion; with increased cloud amount $\partial T/\partial S$ becomes smaller. Due to the strong absorption of solar radiation by clouds deep freeze solutions are possible only for very low values of the solar constant. The response of the model to changes in cloud amount or incoming radiation should be studied as a function of latitude. Two expressions that quantify the sensitivity to changes in the solar constant and cloud amount as a function of latitude are defined. If cloud amount is assumed to increase with temperature in a certain latitude belt and to decrease with temperature elsewhere, $\partial T/\partial S$ (as a function of latitude) and $\partial T/\partial S$ can change considerably.

1. Introduction

The two major effects of atmospheric cloud cover on the earth's climate work in opposing ways. On the one hand, clouds reflect a fraction of the incoming solar radiation and hence cool the earth-atmosphere system; on the other, they absorb outgoing infrared radiation which warms the system. The sign and magnitude of the difference between these two opposing effects is very small compared to the two effects separately (Cess, 1976). However, the imbalance can be very important in determining the earth's climate and its sensitivity to changes in external conditions.

It is obvious that all kinds of feedback loops involving clouds are possible. Many papers on this issue have appeared: for example, diagnostic studies based on zonal climatology (Cess, 1976; Lian and Cess, 1977), more theoretical studies, such as the one by Paltridge (1974), and simulations with general circulation models (Schneider *et al.*, 1978).

In this paper we will investigate the behavior of an EBCM (energy balance climate model) in which cloud amount is incorporated as a parameter. In an earlier paper (Oerlemans and Van den Dool, 1978) we presented a one-dimensional EBCM in which the parameterizations of infrared radiation and albedo were based on a coherent set of satellite data compiled by Ellis and Vonder Haar (1976). This model includes the observed latitudinal distribution of land, sea and topography. The energy balance equation is

$$Q(1 - \alpha) + DV^2T = I, \quad (1)$$

where Q is the incoming solar radiation at the top of the atmosphere, α the planetary albedo, D the diffusion coefficient for total energy, T the sea level temperature and I the outgoing infrared radiation at the top of the atmosphere. If I and α are expressed in terms of T , we can compute the zonally and annually averaged temperature for a given distribution of Q . The sea level temperature is linked to the surface temperature by a constant lapse rate of 6 K km^{-1} .

A serious deficiency of the parameterization used is that only the surface temperature is taken into account explicitly. In the Oerlemans/Van den Dool model the infrared radiation I is related to the surface temperature T_s by

$$I = I_0 + bT_s, \quad (2)$$

where $I_0 = 205 \text{ W m}^{-2}$ and $b = 2.23 \text{ W m}^{-2} \text{ }^\circ\text{C}^{-1}$. This regression relation is derived from the annual mean zonal climatology of I and T_s . Our value for b is large compared to other studies. [For a comparison see Warren and Schneider (1979).] It is obvious that not only T_s changes as a function of latitude but also cloud amount, cloud height, lapse rate, etc. Cloud amount generally increases with latitude which helps to explain the decrease of IR radiation with latitude. Following Cess (1976), we now extend (2) to

$$I = I_0 + bT_s + cA_c, \quad (2a)$$

where A_c is the zonally averaged cloud amount. Al-

TABLE 1. Annual and zonal mean parameters needed for the computation of the albedo. Second column: clear sky albedo taken from Vonder Haar and Ellis (1975); third column: cloud amount according to Berliand and Strokina (1975); fourth column: the same from London (1957). Fifth column: planetary albedo taken from Ellis and Vonder Haar (1976); last two columns: albedo of clouds computed according to Eq. (3).

Latitude	α_s	$A_c(1)$	$A_c(2)$	α_p	$\alpha_c(1)$	$\alpha_c(2)$
-85°S	0.59	0.47	0.47	0.62	0.65	0.65
-75°S	0.53	0.58	0.56	0.60	0.66	0.66
-65°S	0.34	0.83	0.77	0.51	0.55	0.56
-55°S	0.22	0.80	0.79	0.43	0.48	0.48
-45°S	0.16	0.70	0.65	0.36	0.44	0.46
-35°S	0.14	0.59	0.54	0.30	0.40	0.43
-25°S	0.14	0.52	0.47	0.25	0.36	0.38
-15°S	0.14	0.55	0.47	0.24	0.31	0.34
-5°S	0.14	0.58	0.50	0.24	0.31	0.34
5°N	0.15	0.60	0.51	0.25	0.32	0.35
15°N	0.14	0.53	0.44	0.25	0.34	0.38
25°N	0.17	0.47	0.41	0.27	0.39	0.42
35°N	0.18	0.57	0.47	0.31	0.41	0.46
45°N	0.20	0.63	0.57	0.36	0.45	0.47
55°N	0.23	0.71	0.64	0.41	0.48	0.51
65°N	0.30	0.69	0.64	0.45	0.52	0.53
75°N	0.41	0.68	0.61	0.54	0.61	0.63
85°N	0.52	0.70	0.55	0.59	0.62	0.65

though far from perfect, observed climatologies of cloud cover can be used to estimate the coefficient c . The role of the latitudinal variation of cloud altitude, cloud type (stratus versus cumulus mainly) and other parameters is taken into account only implicitly.

A serious limitation is that the lapse rate is not explicitly taken into account in Eq. (2a), though research by Suarez and Held (1979) and others indicates that the variation of the tropospheric stability with latitude causes an increased sensitivity of T to changes in the solar radiation. We tried to express the lapse rate in terms of the fraction of land and the net radiation but the result of this procedure was not convincing.

We will concentrate here on one aspect of clouds—the role of cloud amount in the earth's climate. In Sections 2 and 3 we will discuss the extension of the parameterizations of IR radiation and albedo. In Sections 4 and 5 we will discuss the sensitivity of solutions of the model for changes in cloud amount and incoming radiation, both for the globe as a whole and as a function of latitude.

2. Planetary albedo

The zonally and annually averaged planetary albedo can formally be written as the sum of the clear-sky and cloudy-sky albedos

$$\alpha_p = \alpha_c A_c + \alpha_s(1 - A_c), \quad (3)$$

where A_c is cloud amount and the three albedos α_p , α_c and α_s refer to planetary, cloud and clear sky,

respectively. We have at our disposal observations (zonal climatology) of α_p (Ellis and Vonder Haar, 1976), A_c (Berliand and Strokina, 1975) and α_s (Vonder Haar and Ellis, 1975). Therefore, α_c , the albedo of clouds, can be computed for each latitude. In Table 1 estimates for α_c are given as well as the data on which the estimates are based. For comparison we have also used London's (1957) climatology. The annual mean cloud amount taken from Berliand and Strokina is computed as the average of the four mid-season values.

The A_c estimates of Berliand and Strokina are substantially larger than the earlier estimates by London. To some extent this is due to the use of satellite pictures that tend to show more extensive cloud cover than synoptic methods (Malberg, 1973). Differences in cloud amount, of course, lead to differences in the estimate of α_c . However, as can be seen from Table 1, this effect is rather small. The numerical values of α_c used in the model are given in column 6 of Table 1. The difference between the two hemispheres are insignificant.

We now have determined α_c as a function of latitude. Following Cess (1976), we will interpret this as a zenith angle effect. We neglect any explicit dependence of α_c on T (via cloud type, drop size, etc.).

The clear-sky albedo for land and sea is computed according to the scheme used by Oerlemans and Van den Dool (1978).

The planetary albedo finally reads

$$\alpha_p = \alpha_c A_c + \alpha_{sl} \Delta (1 - A_{cl}) + \alpha_{ss} (1 - \Delta) (1 - A_{cs}), \quad (3a)$$

where A_{cl} and A_{cs} are cloud amount for land and sea (see Table 2), α_{sl} and α_{ss} are the clear-sky albedos for land and sea and Δ is the fraction of land. We note that A_c , A_{cl} , A_{cs} , α_c and Δ are prescribed fixed functions of latitude, whereas α_{sl} and α_{ss} are controlled by T_s . Constants involved in the computations are the albedos over bare land (0.22), sea (0.13), snow (0.61) and ice (0.56).

The albedo computed according to Eq. (3a) for present values of T_s (Table 2) is given as the upper curve in Fig. 1. The agreement with the observed values is good. The lower curve represents the clear-sky albedo, which is computed here as $\alpha_{sl} \Delta + \alpha_{ss} \times (1 - \Delta)$. The differences between both the two hemispheres are clear. In the Northern Hemisphere the clear-sky albedo starts to increase at such a low latitude as 30°, where a small fraction of the land is already covered by snow. We did not incorporate a zenith angle dependence into the clear-sky albedo but this might be too crude (Coakley, 1979).

3. Infrared radiation

With the aid of regression methods the IR radiation can be parameterized in terms of T_s and A_c . Us-

ing infrared data given by Ellis and Vonder Haar (1976), cloud data by Berliand and Strokina (1975) and surface temperatures derived from the 1968–73 data set processed by Oort (1980), we obtain the regression line

$$I = 233 + 2.04T_s - 38.8A_c \text{ [W m}^{-2}\text{]}, \quad (4)$$

where T_s is expressed in °C and A_c as a fraction ($0 < A_c < 1$). As stated in the Introduction the inclusion of cloud amount lowers the proportionality constant b from 2.23 to 2.04. The minus sign of the coefficient of A_c is reasonable, the more clouds the less the outgoing infrared radiation. A similar expression was derived by Cess (1976); with the same satellite data but London's cloud climatology he arrived at

$$I = 257 + 1.6T_s - 91A_c. \quad (4a)$$

This equation holds for the Northern Hemisphere only. It is surprising to see that the coefficients in (4) and (4a) are quite different. In order to investigate this issue we have computed all possible regressions with both cloud climatologies and also with the two sets of surface temperatures.

The first set of temperatures denoted by Oort (Table 2) is obtained from 1000 mb extrapolated to the surface with a lapse rate of 0.006 K m^{-1} . The second, labeled Cess (Table 2), is taken by Cess (1976) from several sources.

The four regressions read are as follows:

$$I = 233 + 2.04T_s^{\text{oort}} - 38.8A_c^{\text{berl}} \quad (4)$$

$$I = 230 + 2.02T_s^{\text{oort}} - 37.8A_c^{\text{lond}} \quad (4b)$$

$$I = 263 + 1.63T_s^{\text{cess}} - 82.8A_c^{\text{berl}} \quad (4c)$$

$$I = 252 + 1.60T_s^{\text{cess}} - 72.2A_c^{\text{lond}}. \quad (4d)$$

In all cases the variance explained by these relations is ~95%. It is obvious that the choice of a particular cloud climatology is not the major cause of the difference between (4) and (4a). Surprisingly, the result

TABLE 2. Annual and zonal mean parameters needed for the computation of albedo and infrared radiation. In the second and third column cloud amount is given for land and sea separately (Berliand and Strokina, 1975). Annual mean values are taken as the average of the four mid-season months. The fourth and fifth columns give two sets of surface temperatures. The first is derived from 1000 mb temperatures as compiled by Oort (1980) for the period 1968–1973; a correction of 0.006 times the height of the land is applied to obtain surface temperatures. The second, $T_s(2)$, is the set of surface temperatures as used by Cess (1976) for similar computations.

Latitude	A_{cl}	A_{cs}	$T_s^{(1)}$	$T_s^{(2)}$
–85°S	0.47	—	–29.3	–43.8
–75°S	0.58	—	–21.2	–33.0
–65°S	—	0.84	–8.8	–6.0
–55°S	—	0.81	1.4	2.8
–45°S	0.54	0.70	8.7	9.7
–35°S	0.42	0.62	14.1	16.6
–25°S	0.37	0.57	19.1	21.4
–15°S	0.52	0.55	23.1	24.6
–5°S	0.63	0.57	24.6	26.2
5°N	0.62	0.59	24.9	26.3
15°N	0.44	0.56	24.3	26.3
25°N	0.36	0.56	19.6	23.2
35°N	0.46	0.61	13.0	15.9
45°N	0.55	0.73	6.2	8.4
55°N	0.66	0.78	0.4	2.2
65°N	0.68	0.70	–5.2	–5.5
75°N	0.65	0.71	–13.4	–12.7
85°N	—	0.70	–18.8	–18.0

is very sensitive to the choice of the surface temperatures. These two sets of surface temperatures (Table 2) differ substantially over Antarctica. We use a "surface" temperature for Antarctica that is ~15°C higher than the observed temperatures used by Cess.

When the two southernmost 10° latitude zones are excluded the expressions (4c) and (4d) come very close to (4) and (4b). Therefore we will use (4) which implies that in our model I depends rather strongly on T_s but rather weakly on A_c .

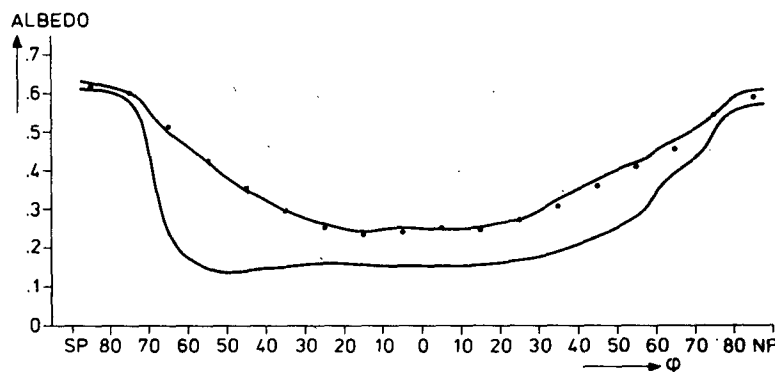


FIG. 1. The planetary albedo computed by the model for present temperatures (upper curve) and the clear sky albedo (lower curve). Dots represent observed values of the planetary albedo (Ellis and Vonder Haar, 1976).

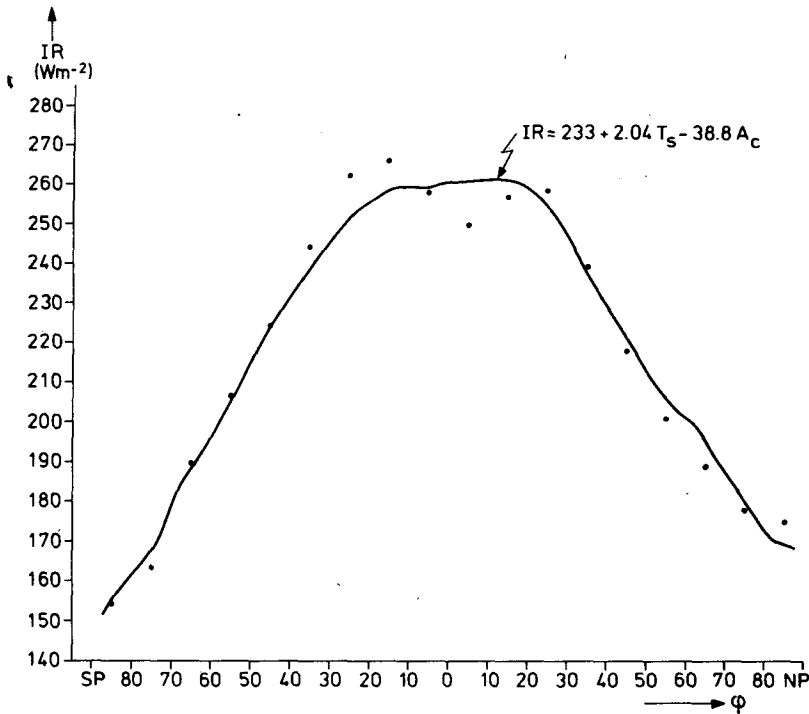


FIG. 2. The infrared emission at the top of the atmosphere computed by the model for present temperatures. Dots represent observed values taken from Ellis and Vonder Haar (1976).

Empirically obtained regression curves always suffer from uncertainties in the determination of the coefficients involved. In this particular case, matters are made worse by the correlation between A_c and T_s . The coefficients obtained from zonal climatology should therefore be used with considerable caution.

From a physical point of view the explicit inclusion of other parameters in (4) would be desirable. For example, it is likely that the lapse rate affects the IR radiation. That is, we might extend (4) to

$$I = I_0 + bT_s + cA_c + d\Gamma, \quad (4e)$$

where $\Gamma (= -\partial T/\partial z)$ is the annual mean lapse rate.

TABLE 3. The global mean sea level temperature ($^{\circ}\text{C}$) computed by the model for different values of the normalized solar constant and normalized cloud amount. The fifth row and the fifth column give the global temperature change for a 1% change in cloud amount and solar constant respectively.

	S			$\frac{S}{100} \frac{\partial \bar{T}}{\partial S}$
	0.99	1.00	1.01	
A_c				
0.95	12.9	14.4	15.9	1.5
1.00	12.4	13.9	15.3	1.45
1.05	11.9	13.3	14.7	1.4
$\frac{A_c}{100} \frac{\partial \bar{T}}{\partial A_c}$	-0.10	-0.11	-0.12	

It can be expected that $d < 0$; as a consequence, b must become larger than 2.04 in order to give the observed latitudinal variation of I . The coefficients in (4) are therefore uncertain because not all of the parameters controlling the IR radiation are included explicitly.

Fig. 2 shows the performance of the IR parameterization for present values of T_s and A_c . There is, of course, a reasonable agreement with the observations. The maximum in the radiation curve is broad and flat. This feature arises because the equatorial zone is characterized by both higher temperatures and more clouds than the subtropics.

4. Results

With the parameterizations discussed in the previous sections we can run the model for present insolation (solar constant $S = 1365 \text{ W m}^{-2}$). The latitudinal distribution of observed temperatures can be reproduced with an accuracy of $\sim 1 \text{ K}$ (not shown). Of course, we can also change the solar constant or cloud amount by some small fraction. In all runs the diffusion coefficient D is taken as $0.7 \text{ W m}^{-2} \text{ K}^{-1}$. Table 3 gives the globally averaged temperature \bar{T} for nine runs of the model.

From Table 3 we can conclude that $\partial \bar{T}/\partial S$, keeping cloud amount fixed, corresponds to 1.45 K for a 1% change in S [more precisely: $(S/100)\partial \bar{T}/\partial S$].

= 1.45 K]. In spite of all changes in the parameterizations this is almost equal to the value of $\partial\bar{T}/\partial S$ in our earlier study (Oerlemans and Van den Dool, 1978). If the snow-ice albedo feedback did not exist, $\partial\bar{T}/\partial S$ would be less (1.15 K). With reduced cloudiness $\partial\bar{T}/\partial S$ becomes larger because the snow-ice albedo feedback is active in a larger area. The runs with fixed solar constant but different cloud amount indicate a small negative value for $\partial\bar{T}/\partial A_c$, of the order of -0.10 K for a 1% change in A_c . Apparently, in our model the increase of the albedo with increasing cloud amount is stronger than the IR reduction. If all clouds are taken away then the global mean temperature rises to about 27°C . On the other hand, a complete global overcast results in a temperature of only 7°C .

In Fig. 3 we have drawn the globally averaged temperature (\bar{T}) for a large range of normalized solar constants. For low values of S we recognize a hysteresis loop as a part of the solution. A comparison of Fig. 3 with Fig. 8 in Oerlemans and Van den Dool (1978) shows the influence of cloud amount. In the earlier version of the model a deep freeze solution existed for solar constants up to 110%. In the present experiment the deep freeze solution exists only for very low values of S . The reason for this change in behavior is clear; due to low cloud albedos (Table 1) at low latitudes the absorption of solar radiation is too high to maintain a completely ice-covered earth. Therefore clouds have a stabilizing effect on the climate for large negative perturbations in S . This stabilizing effect decreases when cloud amount is reduced (Golitsyn and Mokhov, 1978).

So far we have made cloud amount changes that were completely independent from changes in S or T . But suppose that cloudiness were to increase with decreasing temperatures, as is the case in zonal climatology, then cloud amount provides an addi-

tional positive feedback for small perturbations in S . However, we do not know the sign of $\partial A_c/\partial T$ with any confidence and therefore we investigate \bar{T} as a function of S for certain choices of $\partial A_c/\partial T$. In Fig. 4 two solution diagrams are given for $\partial A_c/\partial T = \pm 0.4\% \text{ K}^{-1}$, i.e., a cloud amount change of 0.4% for a 1 K change in T . We take $\partial A_c/\partial T$ to be independent of latitude. The slope of the solution diagram for present insolation ($S = 1$) is somewhat larger if $\partial A_c/\partial T < 0$. For large deviations of the solar constant from its present value the difference between the two runs is pronounced. The lower the value of $\partial A_c/\partial T$ the more the hysteresis loop shrinks and moves to the left. If cloud amount decreases sufficiently fast with temperature the hysteresis loop disappears completely.

5. Local sensitivity of the climate

In Section 4 we have discussed the global mean temperature and the global sensitivity for changes in certain parameters. In the present section we will concentrate on the sensitivity at any given latitude. We will call this local sensitivity in contrast to the term global sensitivity.

The sensitivity of \bar{T} to changes in S is usually (Schneider and Mass, 1975) expressed as

$$S \frac{\partial \bar{T}}{\partial S} = \frac{\bar{I}}{\left(\frac{\partial \bar{I}}{\partial \bar{T}} + \frac{S}{4} \frac{\partial \bar{\alpha}}{\partial T} \right)} \tag{5}$$

In a similar manner we define the local sensitivity by the two expressions

$$Q \left(\frac{\partial T}{\partial Q} \right)_{A_c} = \frac{(1 - \alpha)Q}{\frac{\partial I}{\partial T} + Q \frac{\partial \alpha}{\partial T}} \tag{6}$$

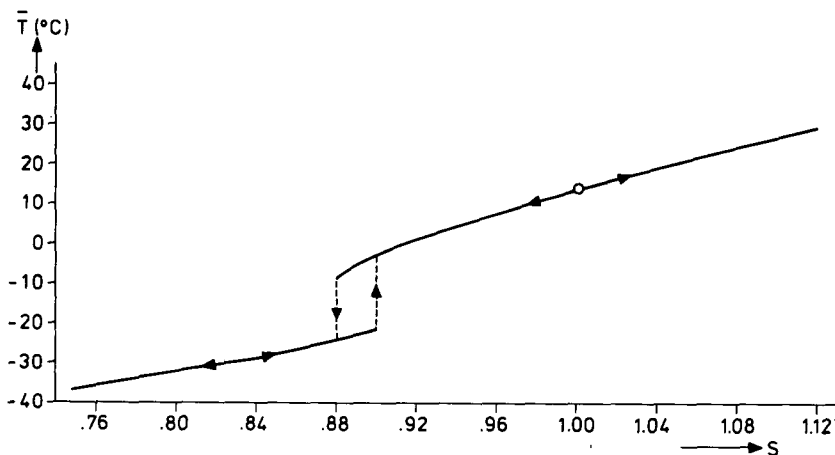


FIG. 3. Solutions of the model, represented by the global mean temperature, for a wide range of normalized solar constants.

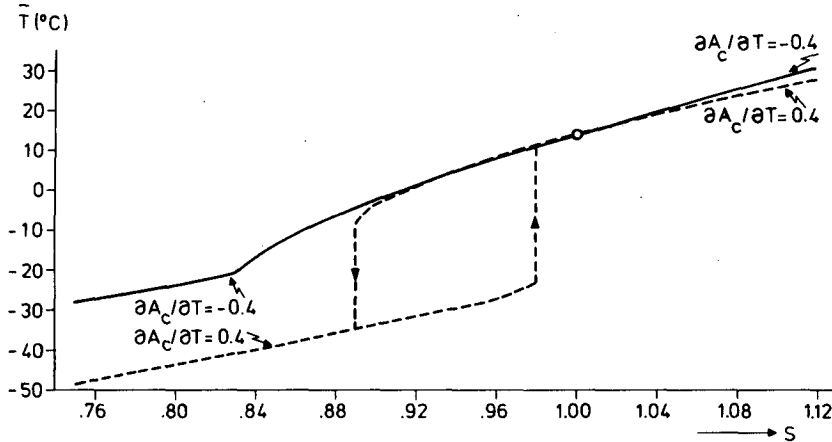


FIG. 4. Solution diagrams for two cases where cloud amount depends on temperature: $\partial A_c/\partial T = -0.4\% \text{ K}^{-1}$ (solid line) and $\partial A_c/\partial T = +0.4\% \text{ K}^{-1}$ (dashed line). [$\partial A_c/\partial T = 0.4\% \text{ K}^{-1}$ means a cloud amount change of 0.4% for a 1 K change in T.]

$$A_c \left(\frac{\partial T}{\partial A_c} \right)_Q = -A_c \frac{Q \frac{\partial \alpha}{\partial A_c} + \frac{\partial I}{\partial A_c}}{\frac{\partial I}{\partial T} + Q \frac{\partial \alpha}{\partial T}}, \quad (7)$$

where Q is the incoming solar radiation at latitude ϕ . These equations express by how much the temperature at latitude ϕ has to change in response to a prescribed change in Q or A_c in order to restore the energy balance. Eqs. (6) and (7) are derived by linearizing (1) under the additional assumption that the horizontal energy transport does not change.

The use of (6) and (7) can increase our insight in the response of the model to changes in either S or A_c . First, we can test the formulas for the albedo and infrared radiation. By looking at a plot of the local sensitivity we decided to simplify one feature of the parameterizations used before; the correction of the

albedo by the introduction of a temperature-dependent woody zone (Oerlemans and Van den Dool, 1978) was skipped because its effect was confusing. Second, we can indicate those latitudes where, according to our parameterizations, potentially large responses exist. Of course, in a model run, it will depend on the formulation of the energy transport whether such large responses really occur at those latitudes or are smoothed out. In our model the value of $\partial T/\partial S$ is fairly independent of latitude despite the effect of the amplifying snow-albedo feedback in a small latitude belt near the -10°C isotherm.

The local sensitivity to changes in Q and A_c is presented in Fig. 5 (full lines). The upper curve gives the temperature change for a 1% change in Q (or S), the lower for a 1% change in A_c . For comparison the dashed lines give the much smoother response of the model to the same changes. (The differences will be discussed below.) The full curve labeled

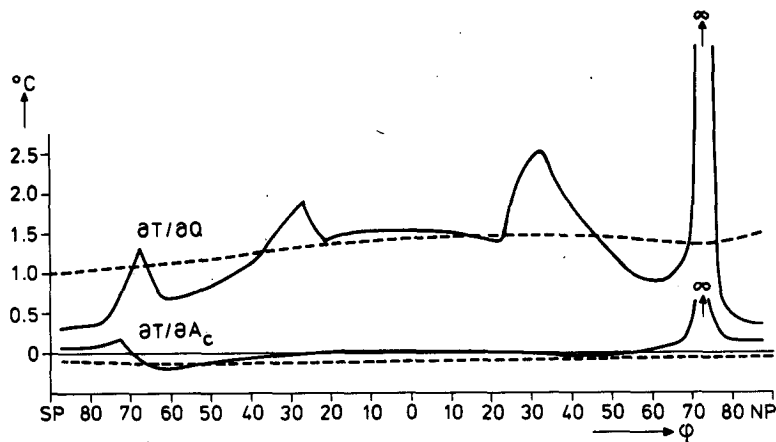


FIG. 5. Local sensitivity as a function of latitude. The upper curve gives the temperature response to a change of 1% in the solar constant [$=(Q/100)(\partial T/\partial Q)$], the lower curve for a change of 1% in cloud amount [$=(A_c/100)(\partial T/\partial A_c)$]. The dashed lines are sensitivities computed by the model.

$\partial T/\partial Q$ indicates clearly the two areas near the -10°C isotherm, namely at 72°N and 67°S . This cannot be a surprise because the 50% ice and snow cover is coupled to this isotherm. But in addition there are sensitive areas at 32°N and 25°S where the land is sufficiently high to have a partial snow cover. There is no doubt that the Northern Hemisphere is potentially much more sensitive to changes in solar radiation than the Southern. In spite of the snow-ice feedback at high latitudes the low latitudes are, in general, more sensitive. There is one latitude zone where a singularity in $\partial T/\partial Q$ shows up; at 70°N there is no way of counterbalancing a drop in Q of 1% by a decrease in IR. The required decrease in IR and thus temperature leads to a large increase in albedo and consequently to a further reduction of absorbed solar radiation, etc.

The full curve labeled $\partial T/\partial A_c$ in Fig. 5 shows a clear dependence on latitude. An increase of A_c by 1% results in a warming over the ice-covered areas whereas at nearly all other latitudes a small cooling takes place. This result agrees with that obtained by Cess (1976). In Section 4 it was stated that an increase of A_c leads to a small global cooling. From Fig. 5 it is evident that this cooling is by no means certain; it seems rather a coincidence that the average is negative. If we had taken into account a small zenith angle dependence for the clear-sky albedo (Coakley, 1979), then $\partial T/\partial A_c$ could have been closer to zero or even positive.

It is interesting to compare the full and dashed lines in Fig. 5. The model's response is much smoother than the response suggested by local sensitivity. The use of a diffusion term in the energy balance (1) tends to degenerate the one-dimensional model to a nearly zero-dimensional model. It would be worthwhile to consider parameterizations of the

horizontal energy flux such that the model's response ($\partial T/\partial S$) can reach much larger values in some areas.

We will now discuss some variations of Fig. 5. Suppose the globe had either less or more cloudiness than at present. With fewer clouds the local sensitivity $\partial T/\partial Q$ becomes larger at higher latitudes; in that case the snow-ice albedo feedback is stronger.

Next, suppose the globe is either colder or warmer than present, while cloud amount remains the same. On the cooler globe the local sensitivity $\partial T/\partial Q$ becomes larger and the maxima shift to the equator. The size of the area where $\partial T/\partial A_c$ is positive becomes larger on a cooler earth. On a deep-freeze earth an increase in cloudiness ultimately leads to warming that increases rapidly toward the equator.

Finally, we consider a case in which cloud amount depends on temperature. How will this affect the local sensitivity to changes in the incoming radiation? Because A_c is allowed to vary we compute (6) without the condition $A_c = \text{constant}$; we denote the result as $Q(dT/dQ)$. Because we do not know the sign of $\partial A_c/\partial T$ we study both $\partial A_c/\partial T = +1$ and $-1\% \text{ K}^{-1}$. The results, in terms of dT/dQ , can be anticipated on the basis of the discussion given above. As shown in Fig. 6, an increase of cloud amount with temperature amplifies dT/dQ over the ice-covered areas whereas a reduced dT/dQ can be found elsewhere. Apparently, the reduction of dT/dQ by the effects of clouds on the albedo dominates the amplification of dT/dQ by the effect of clouds in I , except in areas with a white surface. For negative $\partial A_c/\partial T$ the results are reversed.

In the NCAR general circulation model cloud

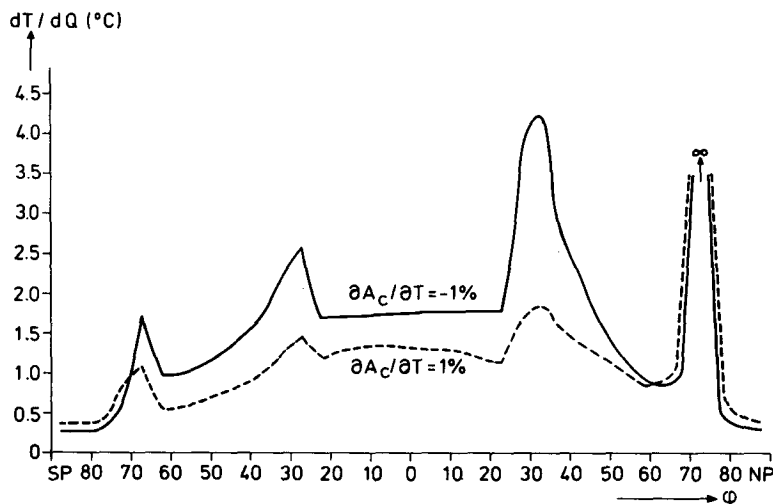


FIG. 6. Local sensitivities $[(Q/100)(dT/dQ)]$ for two cases where cloud amount depends on temperature: $\partial A_c/\partial T = -1\% \text{ K}^{-1}$ (solid line) and $\partial A_c/\partial T = 1\% \text{ K}^{-1}$ (dashed line).

amount at the 3 km level increases poleward of 50°N and decreases equatorward as response to a 2 K higher than normal sea surface temperature (Schneider *et al.*, 1978). The change in cloud cover amounts to several percent. As can be seen from Fig. 6 such a distribution of $\partial A_c/\partial T$ leads to a large amplification of dT/dQ at all latitudes and therefore to a model climate that is extremely sensitive to changes in incoming radiation.

6. Conclusions

Within the limited context of an energy balance climate model we have investigated the role of cloud amount in the sensitivity of the earth's climate. Employing zonal climatology, we derived improved parameterization of albedo and infrared radiation. As a consequence the annual and zonal mean sea level temperature can be reproduced very accurately. Although the relevance of zonal climatology to climate excursions is not entirely certain, we have investigated the model's sensitivity to changes in the solar constant and cloud amount. For the *global* mean temperature (\bar{T}) we have obtained the following conclusions:

- 1) With fixed cloud amount, $(S/100)(\partial\bar{T}/\partial S) \approx 1.45$ K.
- 2) With fixed solar constant, $(A_c/100)(\partial\bar{T}/\partial A_c) \approx -0.1$ K. We consider this sensitivity so small that it can be ignored.
- 3) $\partial\bar{T}/\partial S$ can both be amplified or reduced if we assume that cloud amount depends on temperature in a prescribed way.
- 4) For larger negative changes of S the presence of clouds postpones or prevents deep-freeze solutions of the model.

To study the sensitivity of the climate as a function of latitude we have defined two expressions for local sensitivity [Eqs. (6) and (7)]. These equations express by how much the temperature at latitude ϕ has to change in response to a prescribed change in Q on A_c in order to restore the energy balance. This approach gives more local information than a run with the model. From the calculations of local sensitivity we draw the following conclusions.

- 5) The local sensitivity parameter $\partial T/\partial Q$ generally decreases with latitude. However, this pattern is interrupted at those latitudes where the amount of snow and ice can change quickly. As a whole, the Northern Hemisphere is much more sensitive to changes in Q than the Southern.
- 6) The local sensitivity parameter $\partial T/\partial A_c$ is positive over areas with a white surface and negative elsewhere.
- 7) Both $\partial T/\partial A_c$ and $\partial T/\partial Q$ can differ substantially from their present values on a globe that is either warmer, cooler, more cloudy or less cloudy.

8) If A_c depends on T , the sensitivity parameters change drastically. A model climate extremely sensitive to changes in Q emerges if cloud amount increases (decreases) with temperature at high (low) latitudes.

Acknowledgments. Part of this research was started after discussions with Dr. S. Manabe at GFDL in Princeton. During the course of this study I had many useful discussions with my colleagues Hans Reiff and Hans Oerlemans. I finally thank the reviewers and Drs. H. Tennekes and A. Vernekar who gave editorial advice.

REFERENCES

- Berliand, T. G., and L. A. Strokina, 1975: Cloud regime over the globe. *Tr. Gl. Geofiz. Observ.* **338**, 3–20 (in Russian).
- Cess, R. D., 1976: Climatic change: an appraisal of atmospheric feedback mechanisms employing zonal climatology. *J. Atmos. Sci.*, **33**, 1831–1843.
- Coakley, J. A., 1979: A study of climate sensitivity using a simple energy balance model. *J. Atmos. Sci.*, **36**, 260–269.
- Ellis, J. S., and T. H. Vonder Haar, 1976: Zonal average earth radiation budget measurements from satellites for climate studies. Atmos. Sci. Pap. No. 240, Colorado State University, 46 pp.
- Golitsyn, G. S., and I. I. Mokhov, 1978: Sensitivity estimates and the role of clouds in simple models of climate. *Izv. Atmos. Ocean. Phys.*, **14**, 569–576.
- Lian, M. S., and R. D. Cess, 1977: Energy balance climate models: A reappraisal of ice-albedo feedback. *J. Atmos. Sci.*, **34**, 1058–1062.
- London, J., 1957: A study of the atmospheric heat balance. Report, Contract AF 19(122)-165, College of Engineering, New York University [NTIS No. 117227].
- Malberg, H., 1973: Comparison of mean cloud cover obtained by satellite photographs and ground-based observations over Europe and the Atlantic. *Mon. Wea. Rev.*, **101**, 893–897.
- Oerlemans, J. and H. M. Van den Dool, 1978: Energy balance climate models: Stability experiments with a refined albedo and updated coefficients for infrared emission. *J. Atmos. Sci.*, **35**, 371–381.
- Oort, A. H., 1980: Global atmospheric circulation statistics, 1958–1973. NOAA Prof. Pap. [U.S. Govt. Printing Office] (in preparation).
- Paltridge, G. W., 1974: Global cloud cover and earth surface temperature. *J. Atmos. Sci.*, **31**, 1571–1576.
- Schneider, S. H., and C. Mass, 1975: Volcanic dust, sunspots and temperature trends. *Science*, **190**, 741–476.
- , W. M. Washington and R. M. Chervin, 1978: Cloudiness as a climatic feedback mechanism: Effects on cloud amounts of prescribed global and regional surface temperature changes in the NCAR GCM. *J. Atmos. Sci.*, **35**, 2207–2221.
- Suarez, M. J., and I. M. Held, 1979: The sensitivity of an energy balance climate model to variations in the orbital parameters. *J. Geophys. Res.*, **84**, 4825–4836.
- Vonder Haar, T. H. and J. Ellis, 1975: Albedo of cloud free earth-atmosphere system. *Preprints 2nd Conf. Atmospheric Radiation*, Arlington, Amer. Meteor. Soc., 107–110.
- Warren, S. G., and S. H. Schneider, 1979: Seasonal simulations as a test for uncertainties in the parameterization of a "Budyko-type" climate model. *J. Atmos. Sci.*, **36**, 1377–1391.